FILE COPY
NO. 1677

CASE FILE
COPY

NATIONAL ADVISORY COMMITTEE FOR AERONAUTICS

TECHNICAL NOTE

No. 1677

EXPERIMENTAL AND CALCULATED CHARACTERISTICS OF SEVERAL HIGH-ASPECT-RATIO TAPERED WINGS INCORPORATING NACA 44-SERIES, 230-SERIES, AND LOW-DRAG 64-SERIES AIRFOIL SECTIONS

By Thomas V. Bollech

Langley Aeronautical Laboratory
Langley Field, Va.

DOCUMENT ON LOAN FROM THE FILES OF

NATIONAL ADVISORY COMMITTEE FOR AERONAUTICS
LANGLEY MEMORIAL AERONAUTICAL LABORATORY
LANGLEY FIELD, HAMPTON, VIRGINIA

RETURN TO THE ABOVE ADDRESS.

REQUESTS FOR PUBLICATIONS SHOULD BE ADDRESSED AS FOLLOWS:

NATIONAL ADVISORY COMMITTEE FOR AERONAUTICS
1724 F STREET, N.W.
WASHINGTON 25, D.C.

Washington
September 1948

ERRATUM

NACA TN No. 1677

EXPERIMENTAL AND CALCULATED CHARACTERISTICS OF SEVERAL HIGH-ASPECT-RATIO TAPERED WINGS INCORPORATING NACA 44-SERIES, 230-SERIES, AND LOW-DRAG 64-SERIES AIRFOIL SECTIONS

By Thomas V. Bollech

September 1948

Page 8, line 1: Delete the first six words. The line should then read

"the same for all wings, with only small"

NATIONAL ADVISORY COMMITTEE FOR AERONAUTICS

TECHNICAL NOTE NO. 1677

EXPERIMENTAL AND CALCULATED CHARACTERISTICS OF SEVERAL HIGH-ASPECT-RATIO TAPERED WINGS INCORPORATING NACA 44-SERIES, 230-SERIES, AND LOW-DRAG 64-SERIES AIRFOIL SECTIONS

By Thomas V. Bollech

SUMMARY

The lift, drag, and pitching-moment characteristics of several unswept wings were determined by wind-tunnel tests and by calculations using the method of NACA TN No. 1269. The wings were similar in plan form with aspect ratio 10, taper ratio 2.5, and with root-chord and tip-chord thickness ratios of 20 and 12 percent, respectively. The airfoil sections used were the NACA 44-series, 230-series, and low-drag 64-series.

The aerodynamic characteristics of the wings were determined experimentally for the smooth and rough model conditions with flaps neutral and partial-span and full-span split flaps deflected 60°. The tests were made through a range of Reynolds number from approximately 2.0×10^6 to approximately 5.0×10^6.

A comparison of the calculated and experimental characteristics was made only for the flap-neutral, smooth-model condition and indicates that the agreement obtained in most cases was excellent. No definite trend exists which would indicate that the degree of correlation obtainable depends on airfoil section within the range of variables investigated.

At a constant value of Reynolds number the experimental values of maximum lift coefficients obtained for the smooth models with flaps neutral were approximately equal. With flaps deflected, the highest value of maximum lift coefficient was obtained for the wing of NACA 230-series sections. For the rough model with flaps neutral the greatest loss in maximum lift was experienced by the wing of NACA 230-series sections and the smallest loss was experienced by the wing of NACA 64-series sections. With the flaps deflected and the models in the rough condition, the maximum lift coefficients were approximately equal for all wings. The wing of NACA 64-series sections in the smooth condition exhibited lower minimum drag values and slightly better values

of maximum lift-drag ratios than the wings of NACA 230-series or 44-series sections. In the rough condition, however, all wings produced approximately the same values of maximum lift-drag ratios, and the wing with NACA 230-series sections exhibited the lowest values of minimum drag coefficient. With flaps neutral, the wing of NACA 230-series sections exhibited an abrupt stall, which may be unsatisfactory when stall warning or lateral control at the stall is considered. The stall of the wings with NACA 64-series and 44-series sections was gradual. With flaps deflected 60°, the stall was more abrupt for all wings than with flaps neutral.

INTRODUCTION

An investigation has been undertaken in the Langley 19-foot pressure tunnel to demonstrate the accuracy of the lifting-line theory in predicting the aerodynamic characteristics of unswept wings with moderate to high aspect ratios and to determine the effects of variations in the geometric parameters of the wings on their aerodynamic characteristics. In the first phase of the investigation, reported in reference 1, seven unswept wings having NACA 44-series sections, aspect ratios of 8, 10, and 12, and taper ratios of 2.5 and 3.5 were investigated to determine the effects of aspect ratio, taper ratio, and chord thickness ratio.

In the final phase of the investigation, reported herein, two wings of NACA 230-series and low-drag 64-series sections were tested and the results are compared with those of a wing of NACA 44-series sections and of the same plan form reported in reference 1 to determine the effects of airfoil profile on the wing aerodynamic characteristics. All wings had an aspect ratio of 10, taper ratio of 2.5, and a root-chord thickness ratio of 0.20.

The experimental lift, drag, pitching-moment, and stalling characteristics of wings with and without leading-edge roughness for the flap-neutral and flap-deflected conditions are presented along with the calculated lift, drag, and pitching-moment characteristics of wings without leading-edge roughness for the flap-neutral condition. The wing characteristics were calculated by the generalized method of the lifting-line theory, which allows the use of nonlinear section-lift curves. (See reference 2.)

SYMBOLS

The coefficients and symbols used herein are defined as follows:

C_L lift coefficient (L/qS)

ΔC_L increment of lift coefficient due to flaps

C_D	drag coefficient (D/qS)
C_{D_o}	profile-drag coefficient (D_o/qS)
C_m	pitching-moment coefficient about quarter-chord point of mean aerodynamic chord $\left(\frac{\text{Pitching moment}}{qS\bar{c}}\right)$
$(L/D)_{max}$	maximum lift-drag ratio
R	Reynolds number $\left(\frac{\rho V\bar{c}}{\mu}\right)$
M	Mach number (V/a)
α	angle of attack of the wing root chord, degrees
δ_f	flap deflection, degrees
$dC_L/d\alpha$	slope of lift curve
dC_m/dC_L	slope of pitching-moment curve

where:

L	lift, pounds
D_o	wing profile drag, pounds
D	drag, pounds
V	free-stream velocity, feet per second
a	velocity of sound, feet per second
ρ	mass density of air, slugs per cubic foot
μ	coefficient of viscosity, slugs per foot-second
S	wing area, square feet
q	free-stream dynamic pressure, pounds per square foot $\left(\frac{1}{2}\rho V^2\right)$
$\bar{c}$	mean aerodynamic chord, feet $\left(\frac{2}{S}\int_0^{b/2} c^2 dy\right)$

b wing span, feet

y spanwise distance, feet

c local chord

Subscripts:

max maximum

min minimum

L=0 zero lift

MODELS AND TESTS

Models

The wings were constructed of laminated mahogany. They were of straight tapered plan form with parabolic tips which extended over the outer 5 percent of the semispan. The wings were designed with zero dihedral and zero sweep; that is, the quarter-chord line was perpendicular to the plane of symmetry. The wings had approximately 3° washout at the construction tip. A layout of a typical tapered wing is shown in figure 1.

The wings incorporated the NACA 44-series, 230-series, and low-drag 64-series airfoil sections (fig. 1) with aspect ratio of 10 and taper ratio of 2.5. The 64-series airfoil sections had a design lift coefficient of 0.4. The ratio of the span to root thickness for the wings was 35. The root-section and tip-section thickness ratios were 20 and 12 percent, respectively, for all wings. The geometric characteristics of the test wings are presented in table I. The designation for the wings is formed from numbers representing, consecutively, the taper ratio, aspect ratio, NACA airfoil series, and root-section thickness in percent of wing chord. (See reference 1.)

In preparation for the tests of the smooth model the wings were lacquered and sanded to an aerodynamically smooth finish. In order to simulate a rough-model test condition, a leading-edge roughness established by the Langley two-dimensional low-turbulence pressure tunnel was used. The roughness was obtained by the application of No. 60 (0.011-inch diameter) carborundum grains to a thin layer of diluted shellac along the complete span over a peripheral distance of 8 percent of the chord measured from the leading edge on both upper and lower surfaces.

A split flap was used in all tests when the flaps were deflected. The chord of the flap was 20 percent of the local wing chord. Partial-span and full-span flaps extended 60 and 98 percent of the wing span,

respectively. The flaps were constructed of $\frac{1}{16}$-inch sheet steel which was attached to wooden blocks cut to the desired flap angle and fastened to the wing as shown in figure 1.

Tests

The tests were conducted in the Langley 19-foot pressure tunnel with the models installed in the tunnel as shown in figure 2. The air in the tunnel was compressed to a density of approximately 0.0055 slug per cubic foot. The tests of the wings with flaps neutral were made through a range of Reynolds number from 2.0×10^6 to 4.95×10^6, which corresponds to a range of Mach number from 0.07 to 0.21, respectively. With the exception of wing 2.5-10-44,20, in which the tests of the rough model were made previous to this investigation and were confined to a Reynolds number of 4.45×10^6, the range of Reynolds number for the wings with flaps deflected was from 2.0×10^6 to 4.0×10^6 which corresponds, respectively, to Mach numbers from 0.07 to 0.17.

The lift, drag, and pitching-moment characteristics for both smooth and rough models were determined with flaps neutral and with partial-span and full-span flaps deflected 60° over an angle-of-attack range from -4° through the angle of stall. The profile drag of smooth wings with flaps neutral was also determined by wake-momentum surveys.

Stall studies were made with flaps neutral and deflected, with and without leading-edge roughness, at a Reynolds number of approximately 3.49×10^6 for wings 2.5-10-64,20 and 2.5-10-230,20. For wing 2.5-10-44,20, the stall studies were made at a Reynolds number of 4.61×10^6. The stall progressions were determined by observation of tufts of wool yarn placed at 20, 40, 60, 80, and 90 percent of the chord and spaced 6 inches on the upper surface of the wing.

Corrections for support tare and interference have been applied to all force-test data. Jet-boundary and air-flow-misalinement corrections have been applied to the angle of attack and drag coefficients. An additional tare drag correction has been applied to all drag data, which causes the drag characteristics of wing 2.5-10-44,20 presented herein to be slightly lower than those characteristics presented in reference 1.

CALCULATIONS

The wing lift, drag, and pitching-moment characteristics were calculated by a generalized method of the lifting-line theory which allows the use of nonlinear section-lift curves. The procedure used

for the calculations is given in detail in reference 2. The airfoil section characteristics required for the calculations were obtained in part from reference 3 and in part from unpublished data from the Langley two-dimensional low-turbulence pressure tunnel.

COMPARISON OF EXPERIMENTAL AND CALCULATED RESULTS

The experimental and calculated lift, total drag, profile drag, and pitching-moment characteristics for the flap-neutral conditions are presented in figures 3 to 5 for a Reynolds number of 3.49×10^6, which corresponds to a Mach number of approximately 0.14. Some of the more significant results are summarized in table II.

Drag.- Excellent agreement between the experimental and calculated drag characteristics was obtained at low values of lift coefficient. As the lift coefficient increased, the experimental drag characteristics increased more rapidly than the calculated characteristics; this effect resulted in a divergence of the two drag polars. (See figs. 3 to 5.) For wings 2.5-10-64,20 and 2.5-10-230,20 this divergence occurred at a lift coefficient of approximately 0.2, whereas for wing 2.5-10-44,20 excellent agreement was obtained up to a lift coefficient of approximately 0.9. This same trend is noted, as would be expected, in the comparison of the force-test profile-drag characteristics in which the force-test profile-drag values were obtained by subtracting from the experimental total-drag value, the value of the calculated induced drag. In general, the profile-drag values obtained from force tests have a tendency to be higher throughout the lift range than the results obtained from either wake surveys or calculations. (See parts (b) of figs. 3 to 5.) The agreement obtained between the calculated and wake-survey profile-drag characteristics is excellent. Possible reasons for the discrepancy between the force-test and calculated profile-drag characteristics are (1) errors in corrections for support tare and stream misalinement, (2) inaccuracies in the calculation of induced drag, and (3) the inability to evaluate the drag at wing tips from section data or wake surveys.

As shown in table II, the calculated values of $(L/D)_{max}$ are higher than the experimental values, except in the case of wing 2.5-10-44,20 where the experimental and calculated values agree. The greatest discrepancy occurred for wing 2.5-10-64,20, where the calculated value of $(L/D)_{max}$ is 11 percent higher than the experimental value. This discrepancy at first appears to be excessive; however, after consideration that the discrepancy represents an increment in drag coefficient of approximately 0.0010, the correlation appears to be reasonable.

Lift.- The calculated lift curves predicted quite accurately the angle of attack for maximum lift and the general shape of the experimental-lift curves throughout the range from zero lift to beyond the stall. In

no case did the calculated maximum lift coefficients vary more than 0.05 from the experimental values, with the average discrepancy being 0.03. (See table II.) The calculated and experimental values of the lift-curve slopes for wings 2.5-10-64,20 and 2.5-10-230,20 were in excellent agreement (see table II); however, the calculated lift-curve slope for wing 2.5-10-44,20 was 4 percent lower than the experimental slope. For all wings the agreement between the experimental and calculated angles of zero lift is considered excellent, with the greatest discrepancy of 0.2° obtained for wings 2.5-10-44,20 and 2.5-10-230,20. (See table II.)

Pitching moment.- The calculated and experimental pitching-moment characteristics were in good agreement throughout the lift range. (See figs. 3 to 5.) The largest discrepancy that existed would result in a 2-percent error in the location of the aerodynamic center. (See table II.)

Remarks.- Although the calculated characteristics show some small variations from the experimental characteristics, no definite trend exists within the scope of this investigation which would indicate that the degree of correlation depends on airfoil section.

COMPARISON OF WINGS OF VARIOUS SECTIONS

The experimental aerodynamic characteristics of wings with smooth leading edges for the flaps neutral and the partial-span and full-span flaps deflected 60° are presented in figures 6 to 8 at a Reynolds number of 3.49×10^6. Figures 9 to 11 present the results of wings with rough leading edges for the flaps neutral and the flaps deflected at a Reynolds number of 4.0×10^6. The effect of flaps on the variations of $C_{D_{min}}$, $(L/D)_{max}$, $C_{L_{max}}$, and $\Delta C_{L_{max}}$ with Reynolds number is presented in figures 12 to 15. Table III summarizes some of the more important aerodynamic characteristics at a Reynolds number of 4.0×10^6. The values presented in table III were obtained from plots similar to those shown in figures 12 to 15. The stall progressions of wings with the flaps neutral and deflected are presented in figures 16 to 18. The stall progressions for wings 2.5-10-64,20 and 2.5-10-230,20 are presented at a Reynolds number of 3.49×10^6, whereas the stall progressions for wing 2.5-10-44,20 are for a Reynolds number of 4.61×10^6. Tuft studies made at various Reynolds numbers for wings 2.5-10-64,20 and 2.5-10-230,20 indicated that Reynolds number did not materially affect the manner of stall progression within the range of Reynolds number tested.

Flaps Neutral

Drag.- A general comparison of the wing drag characteristics in figures 6 and 9 for the smooth and rough models indicates that the variations of drag coefficient with lift coefficient were essentially

of maximum lift-drag ratios than the same for all wings, with only small variations occurring in the low and high lift-coefficient range.

A comparison of the minimum drag coefficients $C_{D_{min}}$ obtained for the smooth and rough models in figure 12 indicates that wing 2.5-10-64,20 in the smooth condition exhibited lower values of $C_{D_{min}}$ throughout the range of Reynolds number investigated than either wing 2.5-10-230,20 or 2.5-10-44,20. The application of leading-edge roughness increased the minimum drag coefficient of the wings to values ranging from 150 to 180 percent of the values obtained for the smooth condition. Wing 2.5-10-64,20 underwent the greatest increase in $C_{D_{min}}$ due to roughness, which resulted in its having a slightly greater minimum drag coefficient than wing 2.5-10-230,20 which had the lowest minimum drag coefficient for the rough condition. In contrast to the NACA 230-series and 44-series airfoils, the NACA 64-series airfoils were designed to maintain laminar flow over a large percentage of the chord. It thus appears quite reasonable that the effect of roughness in fixing the transition at the wing leading edge would have a much greater effect on the minimum drag coefficient of a wing of NACA 64-series sections than on the minimum drag coefficient of wings which have sections not especially designed to operate with extensive regions of laminar flow. In both surface conditions, wing 2.5-10-44,20 produced the highest value of $C_{D_{min}}$.

Comparison of the maximum lift-drag ratios $(L/D)_{max}$ (table II) indicates that wing 2.5-10-64,20 in the smooth condition gave somewhat higher values of $(L/D)_{max}$ than either the 2.5-10-230,20 or 2.5-10-44,20 wings. The value of $(L/D)_{max}$ for wing 2.5-10-64,20 is between 3 and 10 percent greater than that obtained for the other wings, as is indicated from experimental and calculated data, respectively. The addition of leading-edge roughness (table III) reduced the value of $(L/D)_{max}$ for all wings approximately 25 percent with the net result that all wings had approximately the same value of $(L/D)_{max}$. The variation of $(L/D)_{max}$ with Reynolds number (fig. 12) for the rough and smooth models indicates that the value of $(L/D)_{max}$ for all wings tends to increase with Reynolds number, with the exception of wing 2.5-10-44,20 in the smooth condition, for which the value $(L/D)_{max}$ remains approximately the same throughout the range of Reynolds number investigated.

Lift.- In general, the shapes of the lift curves (figs. 6 and 9) for wings 2.5-10-44,20 and 2.5-10-64,20 are similar in that both wings exhibit well rounded lift curves, whereas the lift curve exhibited by wing 2.5-10-230,20 was for all practical purposes linear up to the stall. These general lift-curve characteristics are common for both the smooth and rough models.

The maximum lift coefficients of the smooth wings at a Reynolds number of 4.0×10^6 ranged from 1.43 to 1.49 with wing 2.5-10-230,20 having the highest value (table III). In the Reynolds number range from 2.0×10^6 to 4.0×10^6 the values of the maximum lift coefficient increased with Reynolds number for all wings (fig. 13). Beyond a Reynolds number of 4.25×10^6, which corresponds to a Mach number of approximately 0.175, the value of $C_{L_{max}}$ for wing 2.5-10-230,20 decreased with increasing Reynolds number. Tests of a wing incorporating NACA 230-series airfoil sections but having lower ratios of chord thickness than wing 2.5-10-230,20 (reference 4) indicate that the value of the critical Mach number for the first wing was approximately 0.25 and that the maximum lift coefficient decreased as the Mach number was increased beyond this value. Since the critical Mach number decreases with airfoil thickness ratio (reference 5) adverse compressibility effects would be expected to occur at a lower Mach number for wing 2.5-10-230,20 than for the wing described in reference 4. The decrease in maximum lift of wing 2.5-10-230,20 as the Reynolds number is increased beyond 4.25×10^6 is accordingly believed to result from adverse compressibility effects. Although no decrease was obtained in $C_{L_{max}}$ with Reynolds number for the wings of NACA 64- and 44-series sections, the curves of $C_{L_{max}}$ for these wings show a tendency to level off at the higher Reynolds numbers; this condition may be due to less adverse compressibility effects than those which were encountered for the wing of NACA 230-series sections.

The application of leading-edge roughness (fig. 13) greatly reduced the value of maximum lift coefficient for all wings. The decrement in $C_{L_{max}}$ due to roughness at a Reynolds number of 4.0×10^6 for wings 2.5-10-44,20, 2.5-10-64,20, and 2.5-10-230,20 was 0.35, 0.23, and 0.52, respectively. The relatively large decrement in maximum lift coefficient which resulted from the application of roughness to the leading edge of wing 2.5-10-230,20 caused the maximum lift of this wing to be considerably lower than the maximum lifts obtained for the other wings at a Reynolds number of 4.0×10^6. Examination of the data of figure 13 also shows that the decrement in maximum lift coefficient caused by roughness increases somewhat for wing 2.5-10-230,20 at the lower Reynolds numbers, while it remains nearly constant for the other wings. Wing 2.5-10-64,20 showed the highest values of maximum lift throughout the range of Reynolds number investigated. No decrease in $C_{L_{max}}$ with increasing Reynolds number was noted for wing 2.5-10-230,20 in the rough condition. As is pointed out in reference 4, leading-edge roughness reduces the pressure peaks which occur at the leading edge and thus increases the Mach number at which compressibility effects occur.

A comparison of the lift-curve slopes obtained for the smooth wings at a Reynolds number of 4.0×10^6 (table III) indicates that wing 2.5-10-64,20 exhibited the highest lift-curve slope. The values

of lift-curve slope for wings 2.5-10-44,20, 2.5-10-64,20 and 2.5-10-230,20 were 0.0875, 0.0920, and 0.0850, respectively. The addition of leading-edge roughness decreased the lift-curve slopes of the wings by 1 to 6 percent.

The angles of zero lift obtained for smooth wings 2.5-10-44,20, 2.5-10-64,20, and 2.5-10-230,20 were -3.2°, -1.9°, and -0.5°, respectively. (See table III.) Leading-edge roughness did not appreciably affect the angle of zero lift obtained for the smooth condition.

Pitching moment.- The values of pitching-moment coefficients at zero lift for the smooth models (see table III) were -0.096, -0.070, and -0.008 for wings 2.5-10-44,20, 2.5-10-64,20, and 2.5-10-230,20, respectively. The location of the aerodynamic centers were 22, 25, and 26 percent of the mean aerodynamic chord for wings 2.5-10-230,20, 2.5-10-44,20, and 2.5-10-64,20, respectively. In the vicinity of maximum lift a small forward movement of the aerodynamic center was noted for all wings. The application of leading-edge roughness did not appreciably change the wing pitching-moment characteristics.

Stall progression.- As would be expected from the type of lift curves exhibited by the wings, the stall progressions for smooth wings 2.5-10-44,20 and 2.5-10-64,20 were gradual, whereas for wing 2.5-10-230,20 the stall was more or less instantaneous. (See fig. 16.) In the case of wings 2.5-10-44,20 and 2.5-10-64,20, the stall began at the trailing edge of the root section and gradually progressed forward and outboard as the angle of attack was increased. The stall progression for wing 2.5-10-230,20 was more rapid in that no stall was indicated until $C_{L_{max}}$ was reached. At $C_{L_{max}}$ the stall area covered approximately 5 percent of the wing area centered about the trailing edge of the root chord. Just past maximum lift about 75 percent of the wing surface was blanketed in a stalled area. The probability of inadequate stall warning, coupled with the possibility of an asymmetrical stall which would introduce a severe rolling tendency (reference 6), makes it appear likely that the stalling characteristics of wing 2.5-10-230,20 would be unsatisfactory.

The addition of leading-edge roughness did not materially affect the stalling characteristics of the wings, and thus the stall progressions of the roughened wings have not been presented herein. This failure of roughness to affect the stalling characteristics of the wings may be characteristic of the particular airfoil sections employed and the Reynolds number at which the tests were made and should not be construed to be characteristic of other wings or test conditions.

Flaps Deflected

Lift.- The effect of flaps on the wing maximum lift coefficient varied considerably with airfoil section. (See fig. 15.) The increments

in maximum lift coefficient due to full-span flaps for wings 2.5-10-44,20 and 2.5-10-230,20 were 18 and 30 percent greater, respectively, than for wing 2.5-10-64,20; trailing-edge split flaps are thus indicated to be more effective for wings 2.5-10-44,20 and 2.5-10-230,20 than for wing 2.5-10-64,20. With full-span flaps deflected 60°, the maximum lift coefficients obtained at a Reynolds number of 4.0×10^6 were 2.89, 2.71, and 2.47 for wings having NACA 230-series, 44-series, and 64-series sections, respectively. (See fig. 14(b).) Although the values of maximum lift coefficient obtained with partial-span flaps deflected 60° were somewhat lower than those obtained with full-span flaps deflected 60°, the effect of airfoil section was similar. All wings underwent a decrease in maximum lift due to roughness, which was of the same magnitude as that decrease obtained for the flap-neutral condition. In contrast to the low maximum lift coefficient of the roughened 2.5-10-230,20 wing with flaps neutral (fig. 13), the maximum lift coefficient of the 2.5-10-230,20 wing with flaps deflected was, because of its increased flap effectiveness, of the same order of magnitude as $C_{L_{max}}$ obtained for the other wings.

The effect of Reynolds number on $C_{L_{max}}$ (fig. 14) was more pronounced for the smooth condition than for the rough condition. In all cases for which data were available, $C_{L_{max}}$ increased with Reynolds number throughout the range of Reynolds number investigated.

Pitching moment.- In all cases, the 2.5-10-44,20 wing exhibited the highest value of pitching moment, whereas the 2.5-10-230,20 and 2.5-10-64,20 wings exhibited approximately equal values of pitching moment (figs. 7, 8, 10, and 11). A comparison of figures 6 to 11 indicates that the largest trim change due to flap deflection would be obtained for wing 2.5-10-230,20.

Stall progression.- The stall progressions of the wings with flaps deflected were similar to those with flaps neutral in that a root-section stall was predominant in every case. With flaps deflected the stall of all wings was more abrupt than with flaps neutral.

With partial-span flaps deflected 60° (fig. 17), flow separation first occurred just outboard of the flaps. As the angle of attack was increased, the stall spread inboard for wing 2.5-10-44,20. In the case of wings 2.5-10-230,20 and 2.5-10-64,20, no separation occurred on the inboard sections until the angle of attack was increased beyond $C_{L_{max}}$.

The stall progression for the wings with full-span flaps deflected 60° (fig. 18) indicated that no flow separation occurred in the low and moderate angle-of-attack range. In the vicinity of $C_{L_{max}}$, separation occurred rather abruptly over the wing center section.

CONCLUSIONS

The aerodynamic characteristics of several unswept tapered wings were determined by calculations using the method of NACA TN No. 1269 and by wind-tunnel tests to demonstrate the accuracy of calculations and to show the effect of airfoil section on the aerodynamic characteristics of unswept tapered wings. The wings investigated were similar in plan form, had aspect ratio 10 and taper ratio 2.5, and incorporated NACA 44-series, 230-series, and low-drag 64-series airfoil profiles. On the basis of comparison at equal values of Reynolds number the following conclusions were made:

1. The agreement obtained between the calculated and experimental characteristics was in most cases excellent. No definite trend existed within the scope of the investigation which would indicate that the degree of correlation depends on airfoil section.

2. The maximum lift coefficients obtained for the smooth wings with flaps neutral were approximately equal. With flaps deflected and smooth surfaces, the highest value of maximum lift coefficient was obtained for the wing of NACA 230-series sections. Because of the low flap effectiveness for the wing of NACA 64-series sections, the maximum lift coefficient obtained for this wing was lower than that obtained for the wing of NACA 44-series sections and considerably lower than that obtained for the wing of NACA 230-series sections.

3. The greatest loss in maximum lift due to roughness was experienced by the wing of NACA 230-series sections and the smallest loss was experienced by the wing of NACA 64-series sections. Thus for the roughened wings with flaps neutral, the maximum lift coefficient for the wing of NACA 230-series sections was appreciably lower than that obtained from either of the other two wings, and with flaps deflected all wings produced approximately equal values of maximum lift coefficient.

4. The wing of NACA 230-series sections with the flaps neutral exhibited an abrupt stall, which may be unsatisfactory when stall warning or lateral stability at the stall is considered. The stall of the wings with NACA 64-series and 44-series sections was gradual. With flaps deflected 60° all wings stalled more abruptly than with flaps neutral.

5. The wing of NACA 64-series sections in the smooth condition exhibited lower minimum drag values and slightly better values of maximum lift-drag ratios than the wings of NACA 230-series or 44-series sections. In the rough condition, the maximum lift-drag ratios for

all wings were approximately equal, and the wing with NACA 230-series sections exhibited the lowest value of minimum drag coefficient.

Langley Aeronautical Laboratory
National Advisory Committee for Aeronautics
Langley Field, Va., April 22, 1948

REFERENCES

1. Neely, Robert H., Bollech, Thomas V., Westrick, Gertrude C., and Graham, Robert R.: Experimental and Calculated Characteristics of Several NACA 44-Series Wings with Aspect Ratios of 8, 10, and 12 and Taper Ratios of 2.5 and 3.5. NACA TN No. 1270, 1947.

2. Sivells, James C., and Neely, Robert H.: Method for Calculating Wing Characteristics by Lifting-Line Theory Using Nonlinear Section Lift Data. NACA TN No. 1269, 1947.

3. Abbott, Ira H., von Doenhoff, Albert E., and Stivers, Louis S., Jr.: Summary of Airfoil Data. NACA ACR No. L5C05, 1945.

4. Furlong, G. Chester, and Fitzpatrick, James E.: Effects of Mach Number and Reynolds Number on the Maximum Lift Coefficient of a Wing of NACA 230-Series Airfoil Sections. NACA TN No. 1299, 1947.

5. Cleary, Harold E.: Effects of Compressibility on Maximum Lift Coefficients for Six Propeller Airfoils. NACA ACR No. L4L21a, 1945.

6. Pringle, G. E., Francis, R. H., and Birch, A. W. G.: Tests of the Effect of Wing-Tip Section on Stalling Properties of a Low-Wing Monoplane. R. & M. No. 2061, British A.R.C., June 1941.

TABLE I

GEOMETRIC CHARACTERISTICS OF TEST WINGS

Wing	Taper ratio	Aspect ratio	NACA airfoil		Span (ft)	Area (sq ft)	M.A.C. (ft)	Geometric washout (deg)
			Root section	Tip section				
2.5-10-44,20	2.5	10.05	4420	4412	15	22.393	1.592	3.5
2.5-10-64,20	2.5	10.05	64_4-420	64_1-412	15	22.393	1.592	3.0
2.5-10-230,20	2.5	10.05	23020	23012	15	22.393	1.592	3.0

TABLE II

COMPARISON OF EXPERIMENTAL AND CALCULATED RESULTS FOR WINGS

IN SMOOTH CONDITION WITH FLAPS NEUTRAL

$\left[R = 3.49 \times 10^6\right]$

Wing	$C_{D_{min}}$		$(L/D)_{max}$		$C_{L_{max}}$		$\frac{dC_L}{d\alpha}$	
	Calculated	Experimental	Calculated	Experimental	Calculated	Experimental	Calculated	Experimental
2.5-10-44,20	0.0083	0.0083	32.0	32.0	1.41	1.43	0.0827	0.0860
2.5-10-64,20	.0068	.0069	35.4	32.0	1.37	1.40	.0910	.0920
2.5-10-230,20	.0078	.0078	32.2	30.7	1.40	1.45	.0830	.0835

Wing	$\alpha_{L=0}$ (deg)		$(C_m)_{L=0}$		$\left(\frac{dC_m}{dC_L}\right)_{L=0}$	
	Calculated	Experimental	Calculated	Experimental	Calculated	Experimental
2.5-10-44,20	-3.0	-3.2	-0.087	-0.096	0.006	0
2.5-10-64,20	-2.1	-2.0	-.064	-.068	-.025	-.011
2.5-10-230,20	-0.3	-0.5	-.005	-.010	.015	.034

TABLE III

COMPARISON OF EXPERIMENTAL CHARACTERISTICS FOR WINGS

WITH SMOOTH AND ROUGH LEADING EDGES

$\left[R = 4.0 \times 10^6\right]$

Wing	$C_{L_{max}}$						$\frac{dC_L}{d\alpha}$	
	Flaps neutral		Partial-span flaps deflected 60°		Full-span flaps deflected 60°		Flaps neutral	
	Smooth	Rough	Smooth	Rough	Smooth	Rough	Smooth	Rough
2.5-10-44,20	1.44	1.08	2.35	-----	2.71	-----	0.0875	0.0820
2.5-10-64,20	1.43	1.20	2.22	1.92	2.47	2.22	.0920	.0880
2.5-10-230,20	1.49	.97	2.47	1.94	2.89	2.32	.0850	.0840

Wing	$\alpha_{L=0}$ (deg)		$(L/D)_{max}$		$C_{D_{min}}$		$(C_m)_{L=0}$		$\left(\frac{dC_m}{dC_L}\right)_{L=0}$	
	Flaps neutral		Flaps neutral		Flaps neutral		Flaps neutral		Flaps neutral	
	Smooth	Rough	Smooth	Rough	Smooth	Rough	Smooth	Rough	Smooth	Rough
2.5-10-44,20	-3.2	-2.8	31.4	23.7	0.0082	0.0133	-0.096	-0.092	0	0.021
2.5-10-64,20	-1.9	-1.8	32.1	24.0	.0070	.0125	-.070	-.065	-.011	-.011
2.5-10-230,20	-.5	-.5	31.4	23.3	.0078	.0118	-.008	-.008	.035	.036

NACA

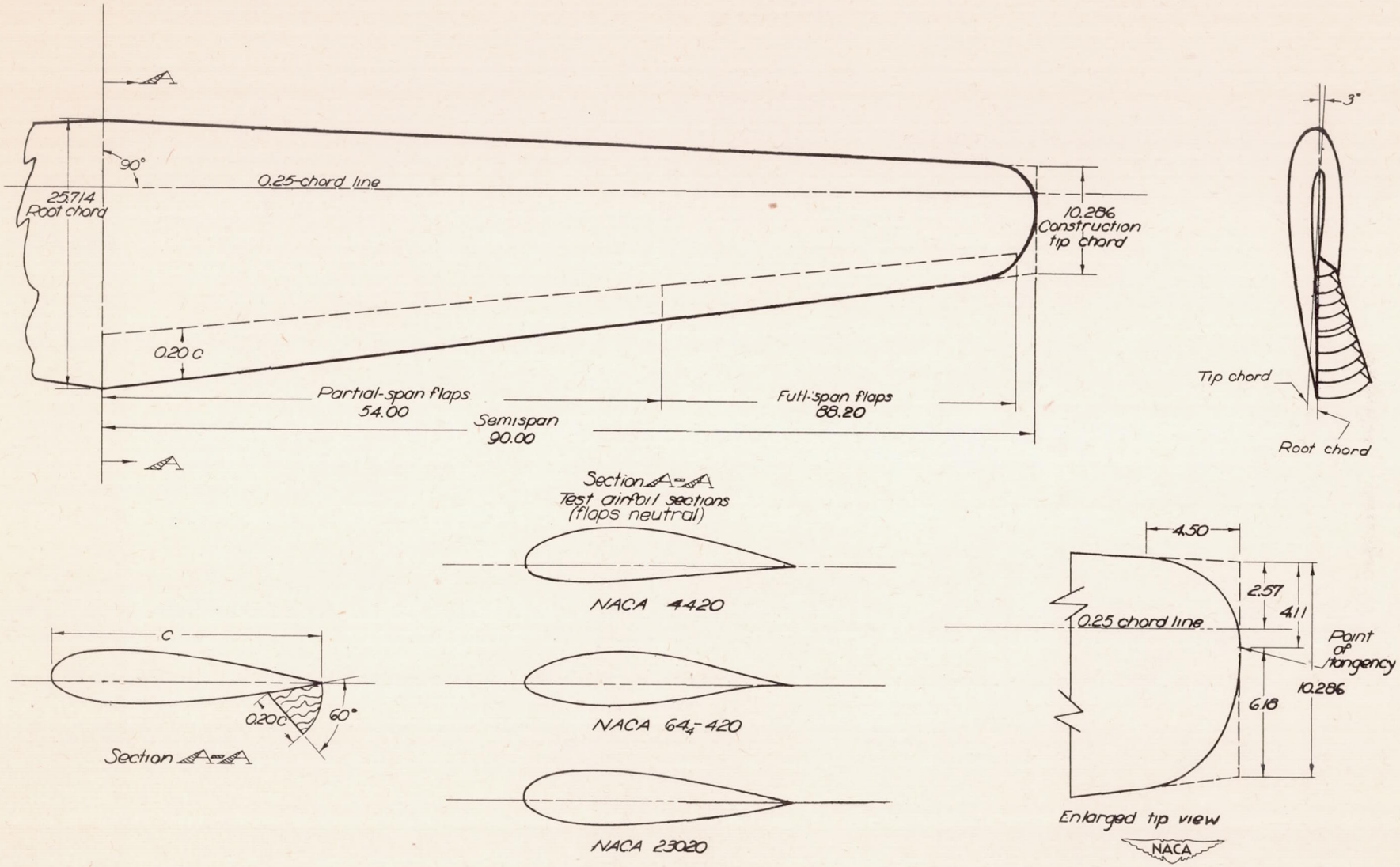

Figure 1.- Layout of typical tapered wing. (All dimensions in inches.)

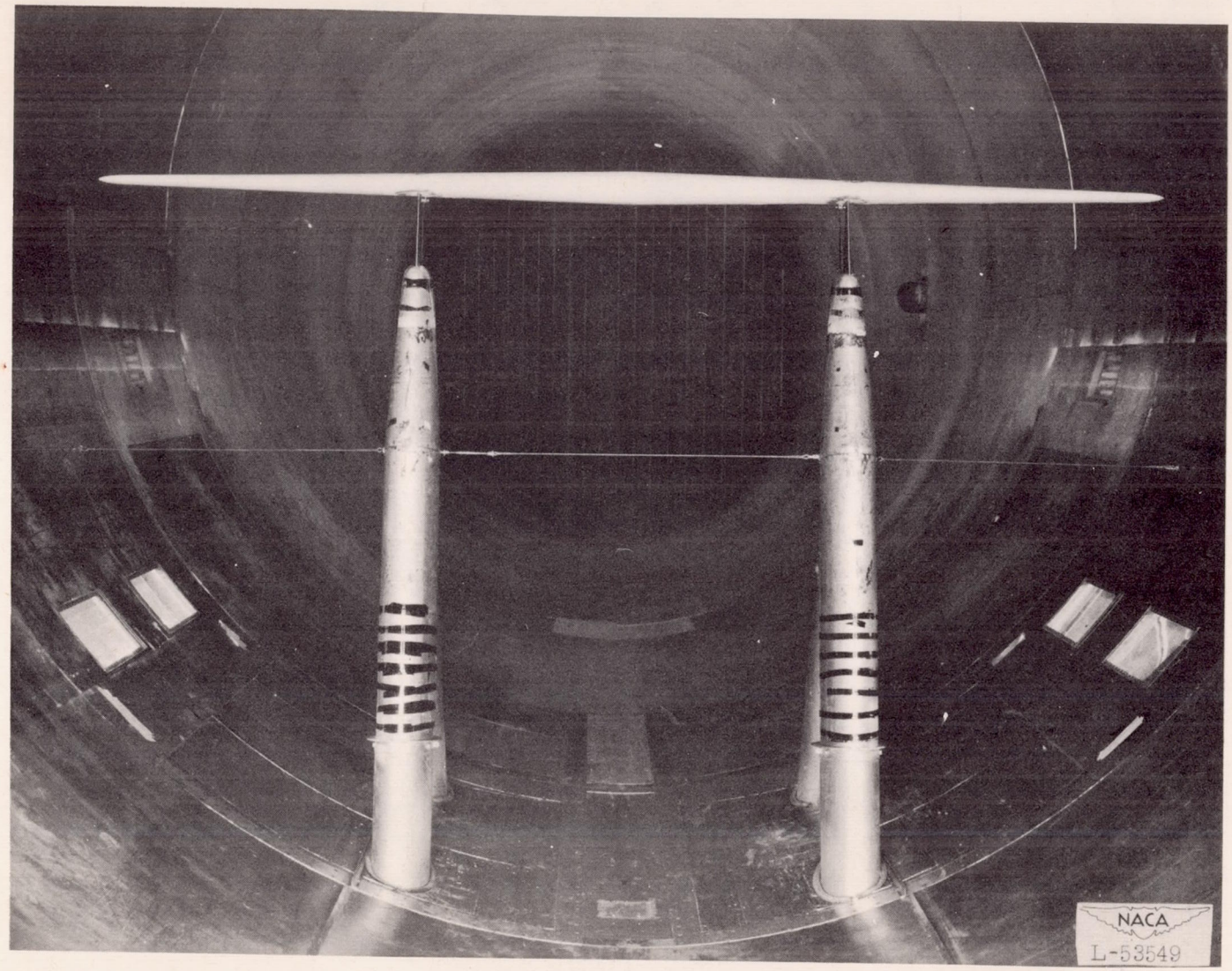

Figure 2.- High-aspect-ratio tapered wing mounted in the Langley 19-foot pressure tunnel.

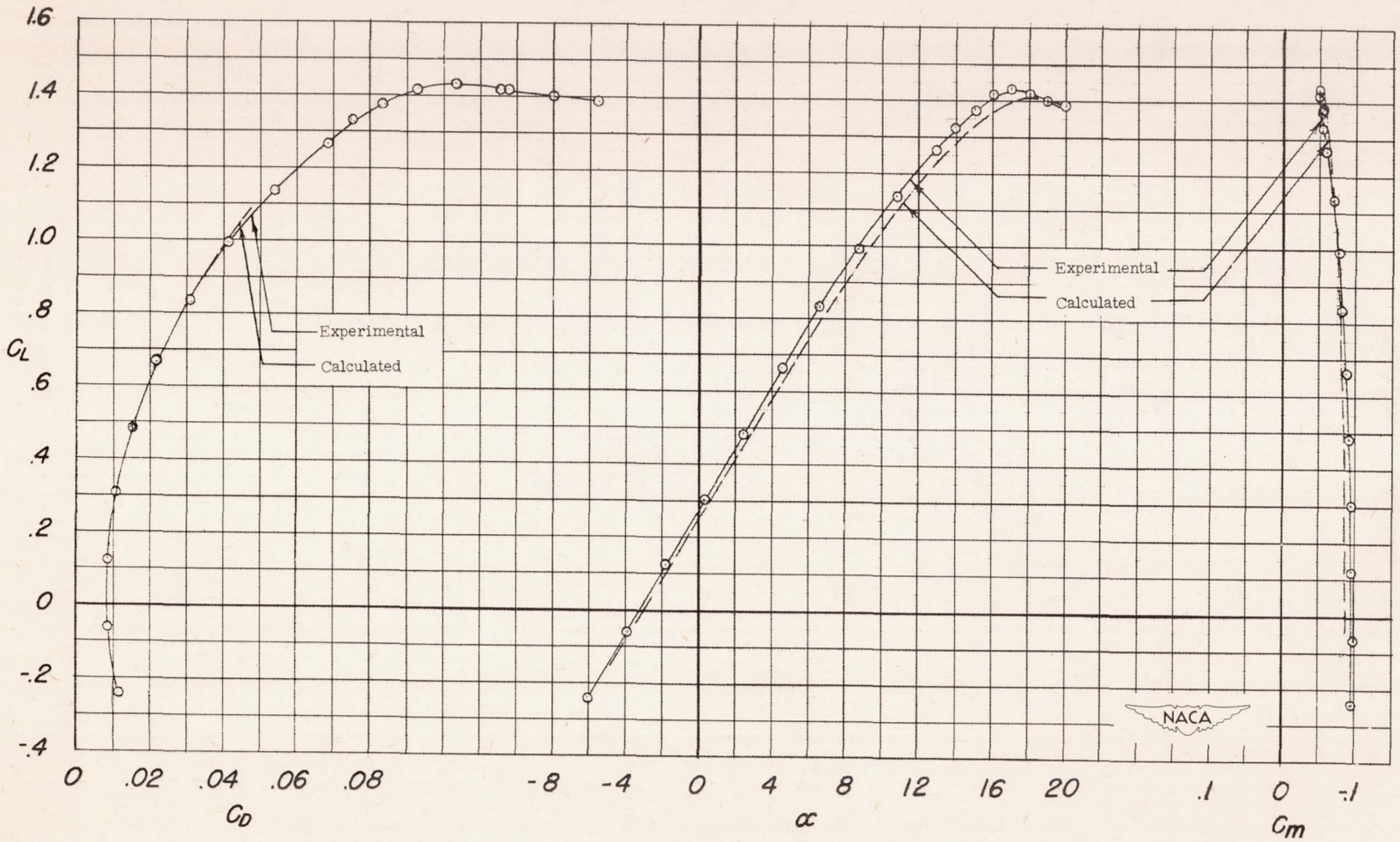

(a) C_L against C_D, α, and C_m.

Figure 3.- Experimental and calculated characteristics of wing 2.5-10-44,20 with smooth leading edge. Flaps neutral. $R = 3.49 \times 10^6$.

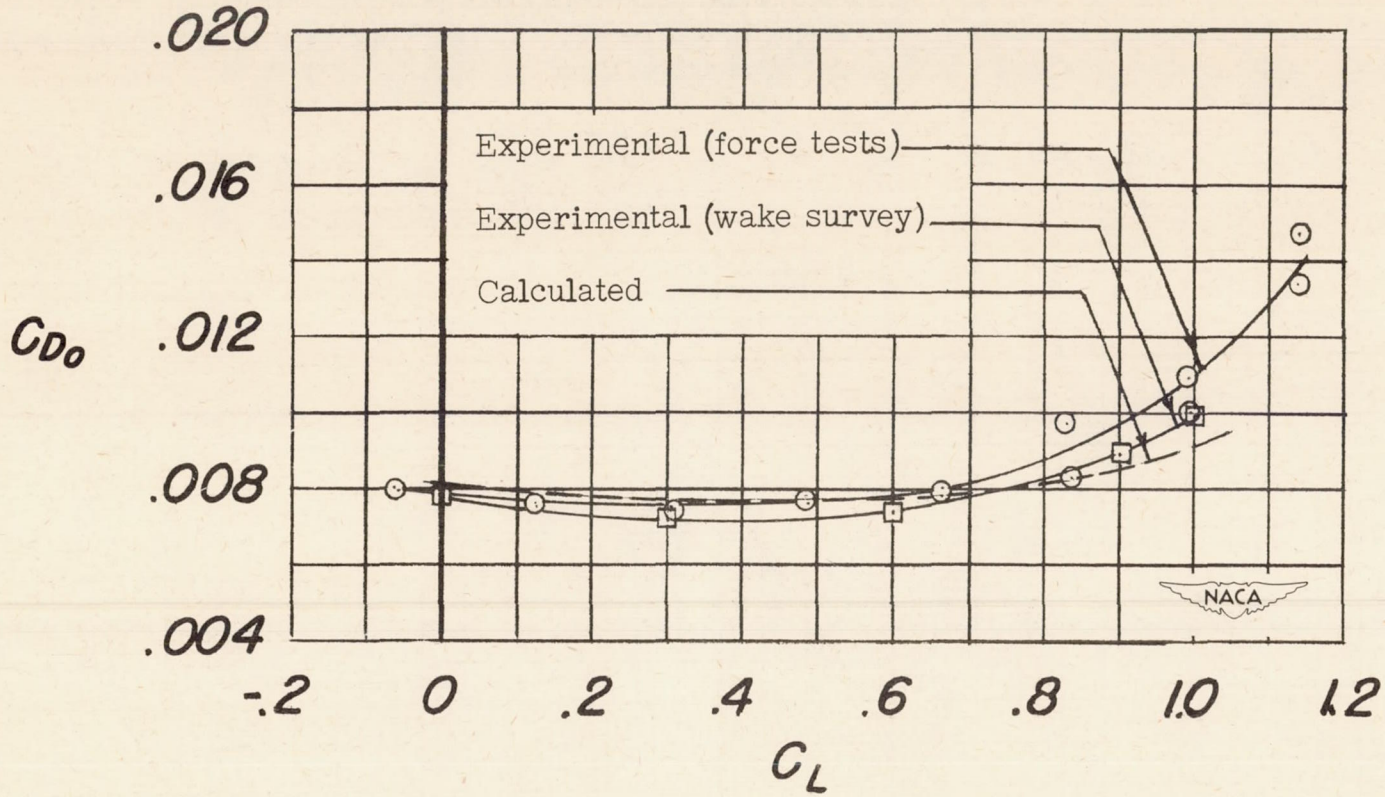

(b) C_{D_o} against C_L.

Figure 3.- Concluded.

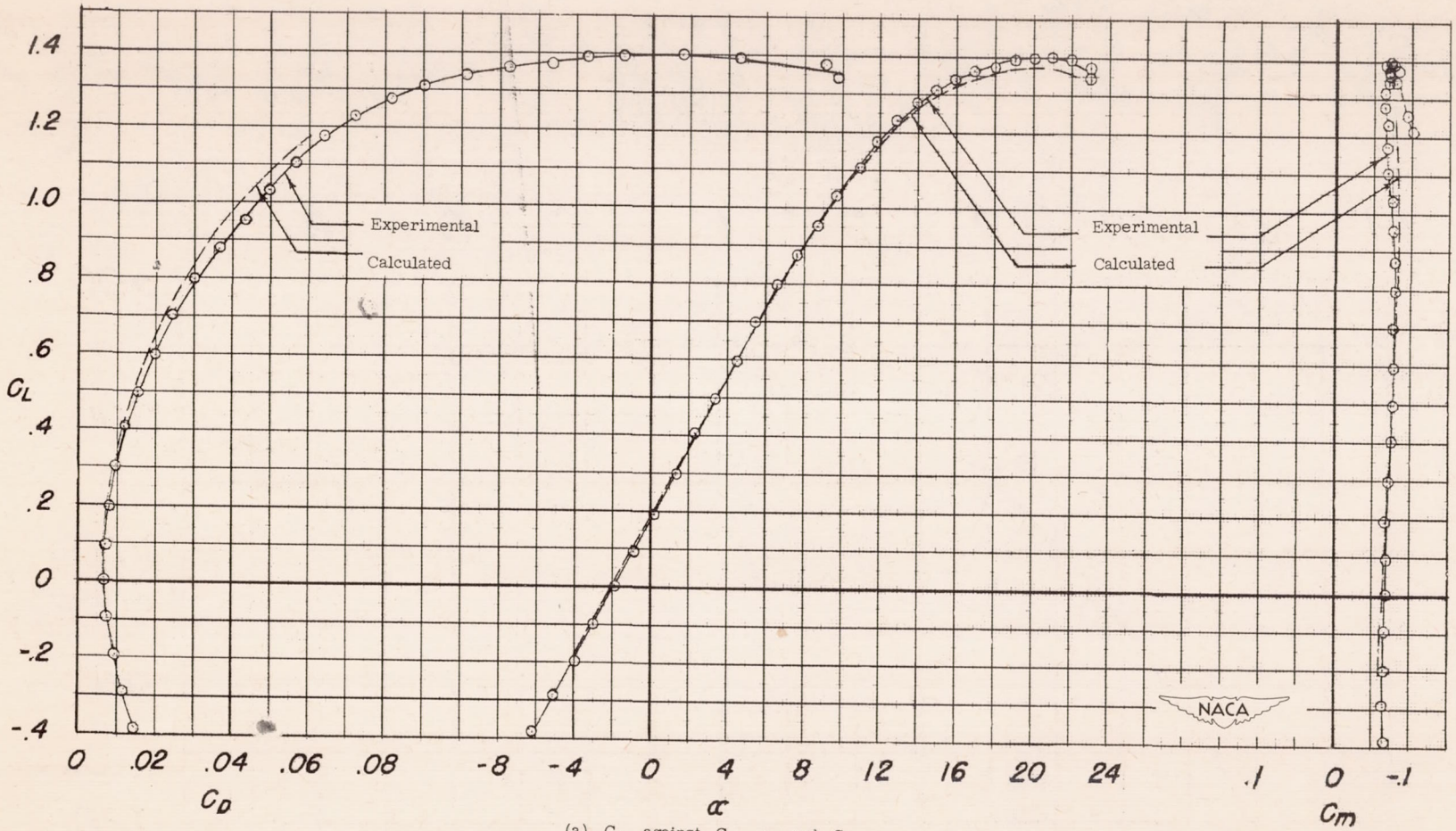

(a) C_L against C_D, α, and C_m.

Figure 4.- Experimental and calculated characteristics of wing 2.5-10-64,20 with smooth leading edge. Flaps neutral; $R = 3.49 \times 10^6$.

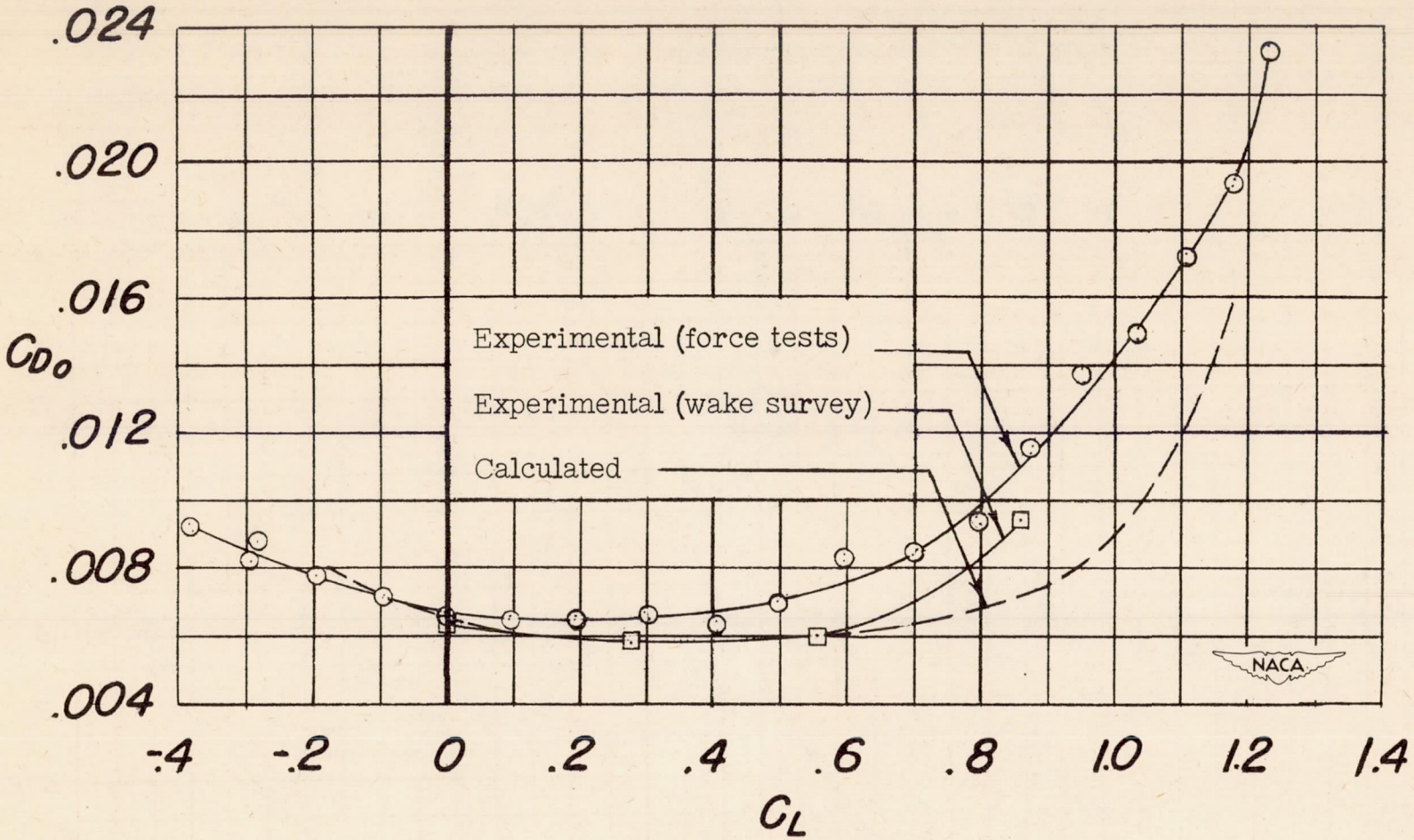

(b) C_{D_o} against C_L.

Figure 4.- Concluded.

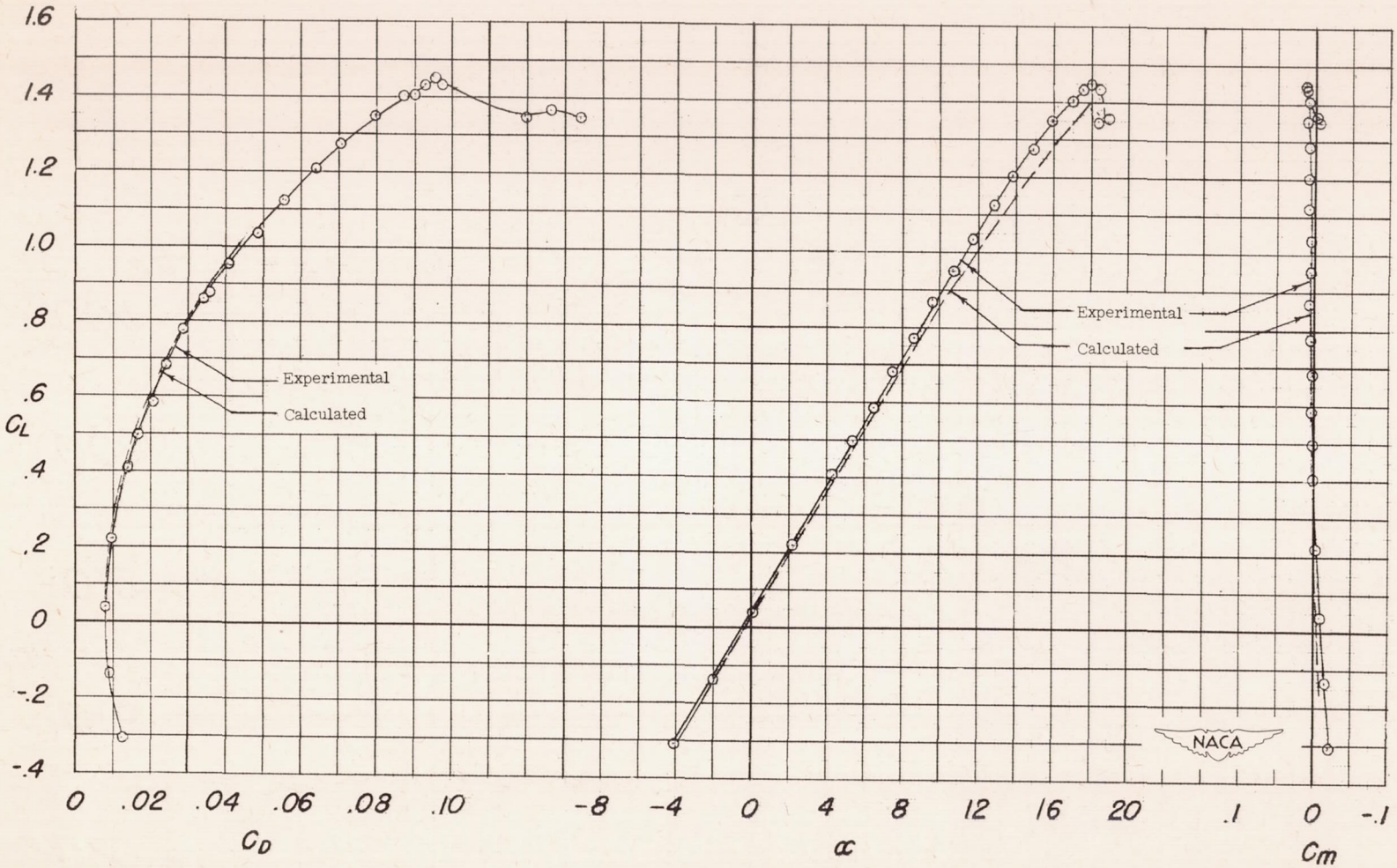

(a) C_L against C_D, α, and C_m.

Figure 5.- Experimental and calculated characteristics of wing 2.5-10-230,20 with smooth leading edge. Flaps neutral; $R = 3.49 \times 10^6$.

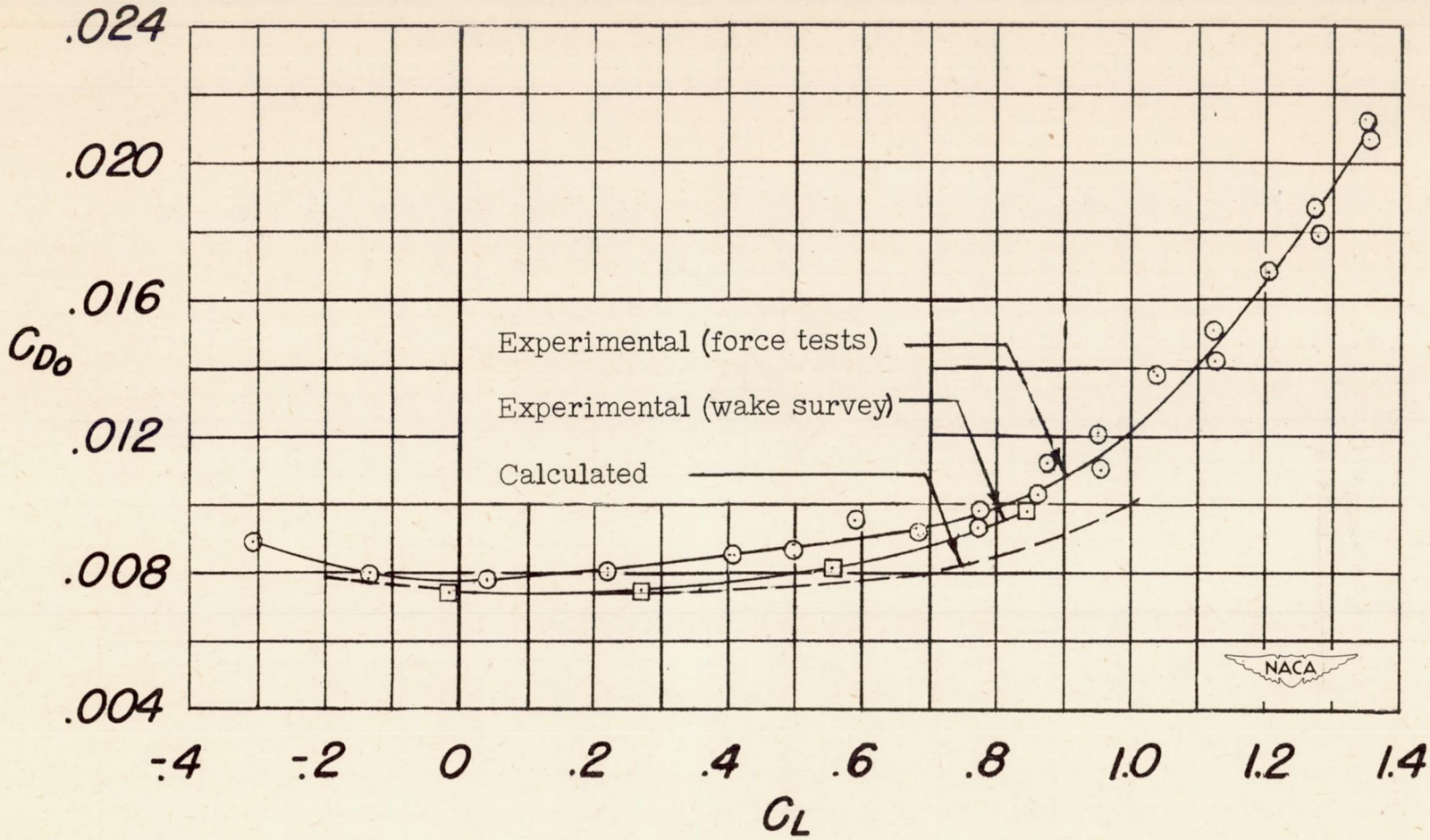

(b) C_{D_o} against C_L.

Figure 5.- Concluded.

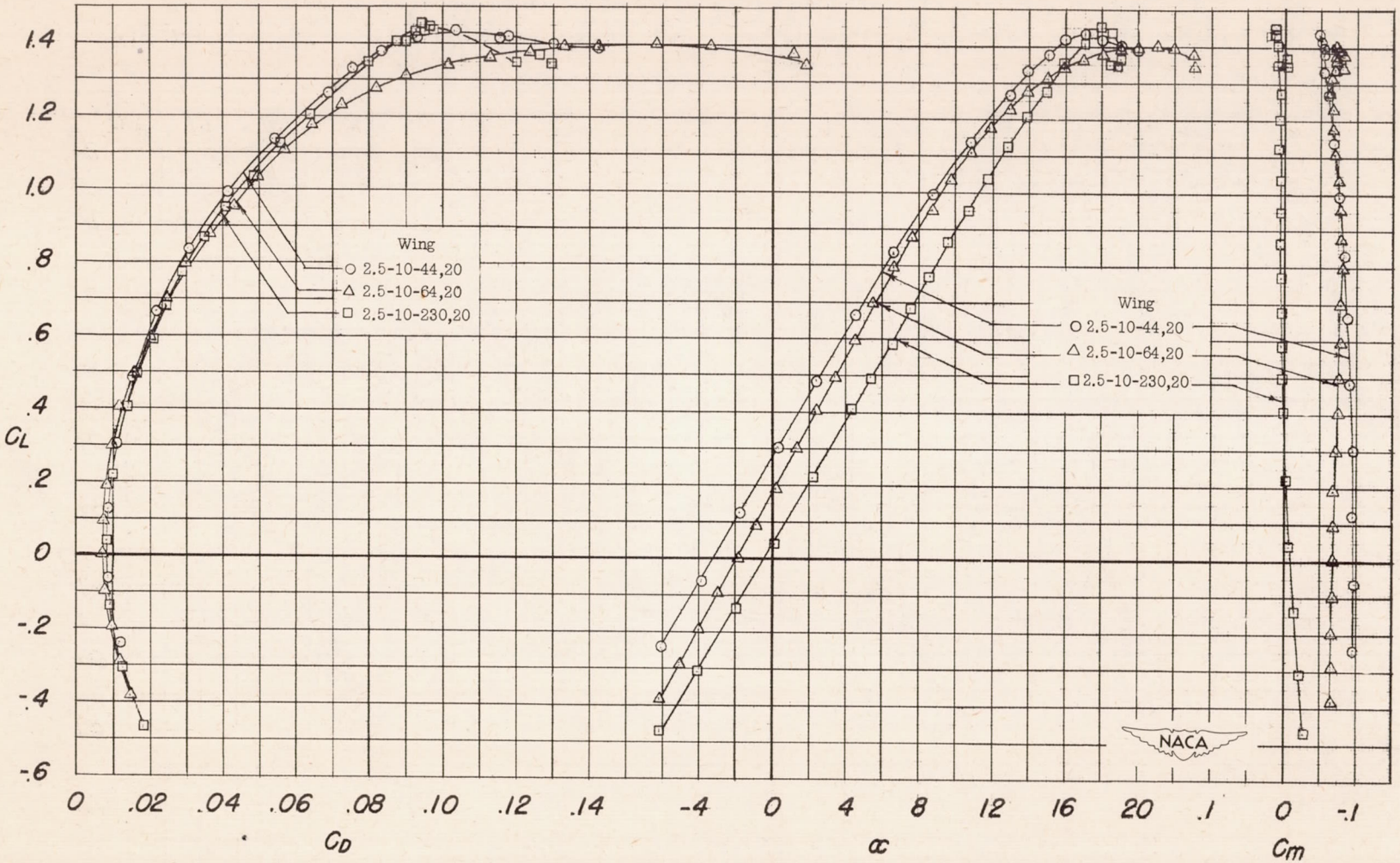

Figure 6.- Effect of airfoil section on the characteristics of wings with smooth leading edge. Flaps neutral; $R = 3.49 \times 10^6$.

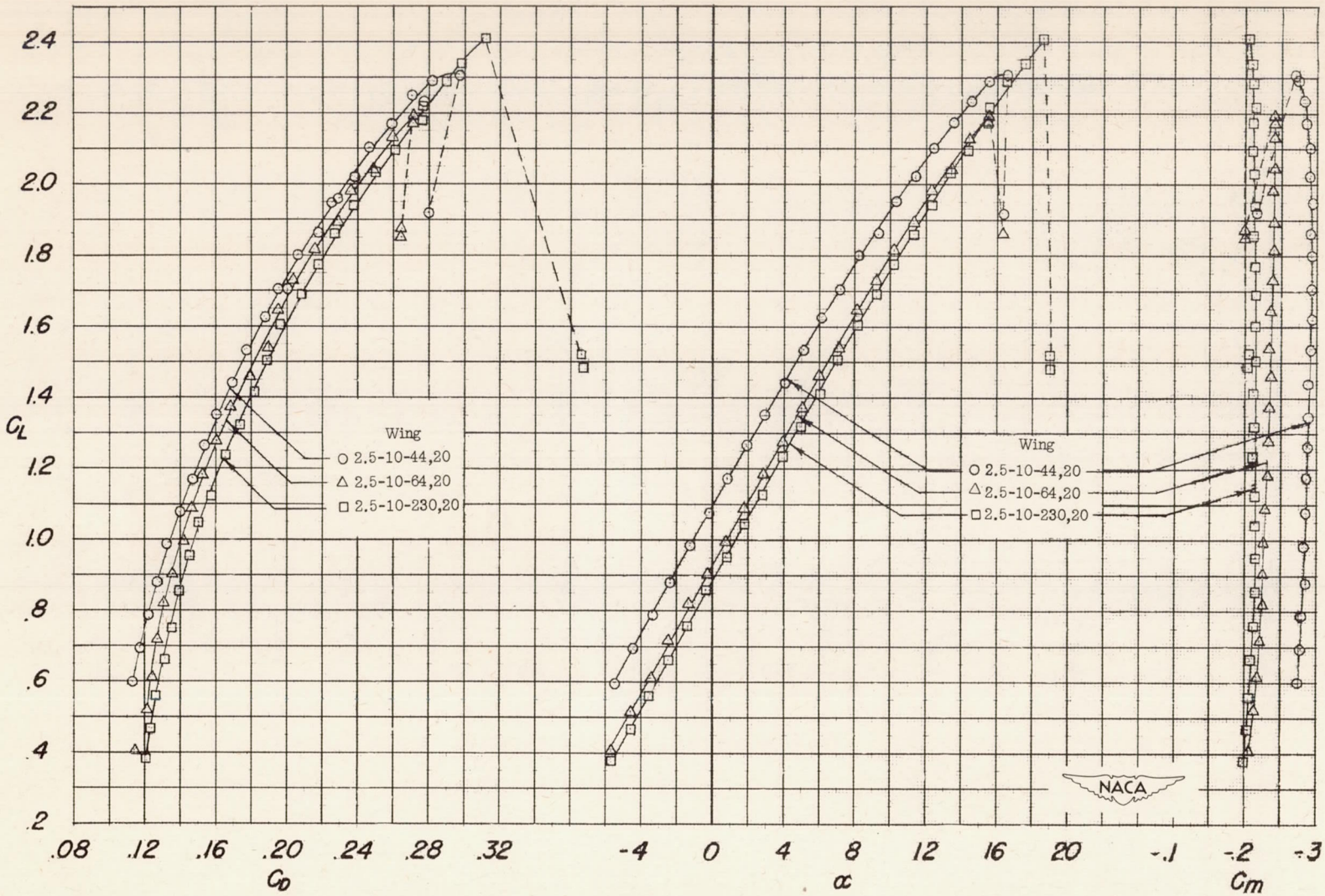

Figure 7.- Effect of airfoil section on the characteristics of wings with smooth leading edge. Partial-span flaps deflected 60°; $R = 3.49 \times 10^6$.

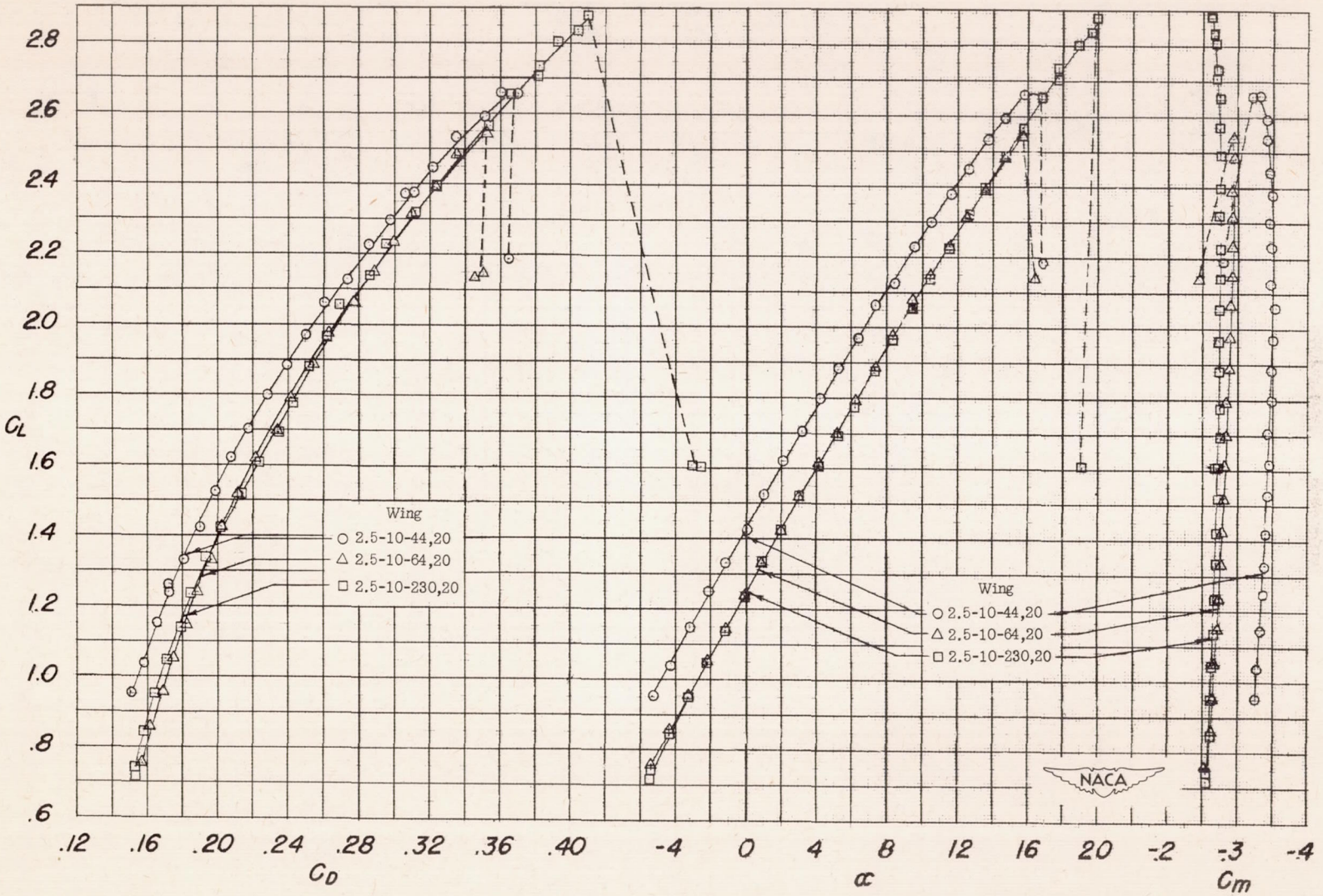

Figure 8.- Effect of airfoil section on the characteristics of wings with smooth leading edge. Full-span flaps deflected 60°; $R = 3.49 \times 10^6$.

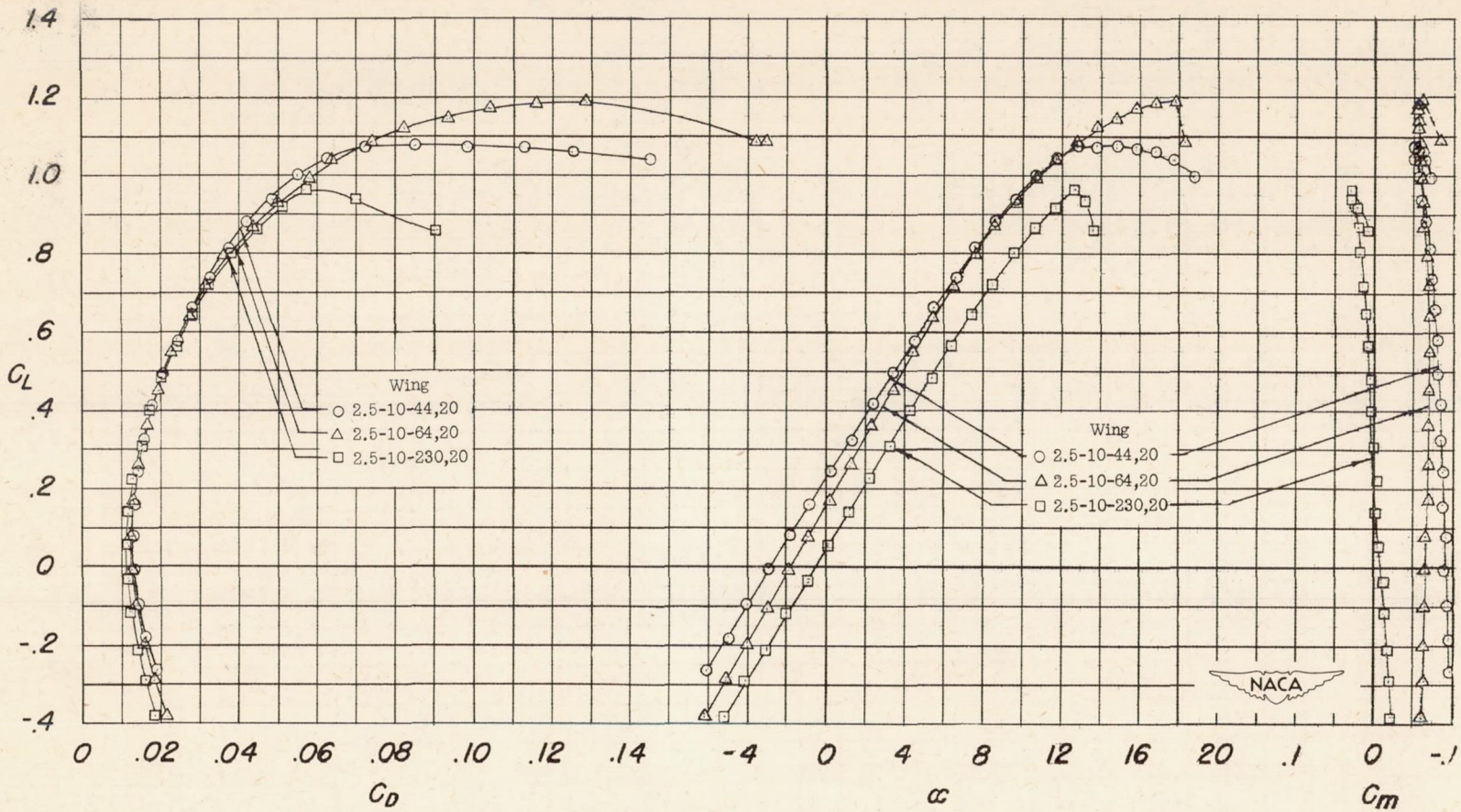

Figure 9.- Effect of airfoil section on the characteristics of wings with rough leading edge. Flaps neutral; $R = 4.0 \times 10^6$.

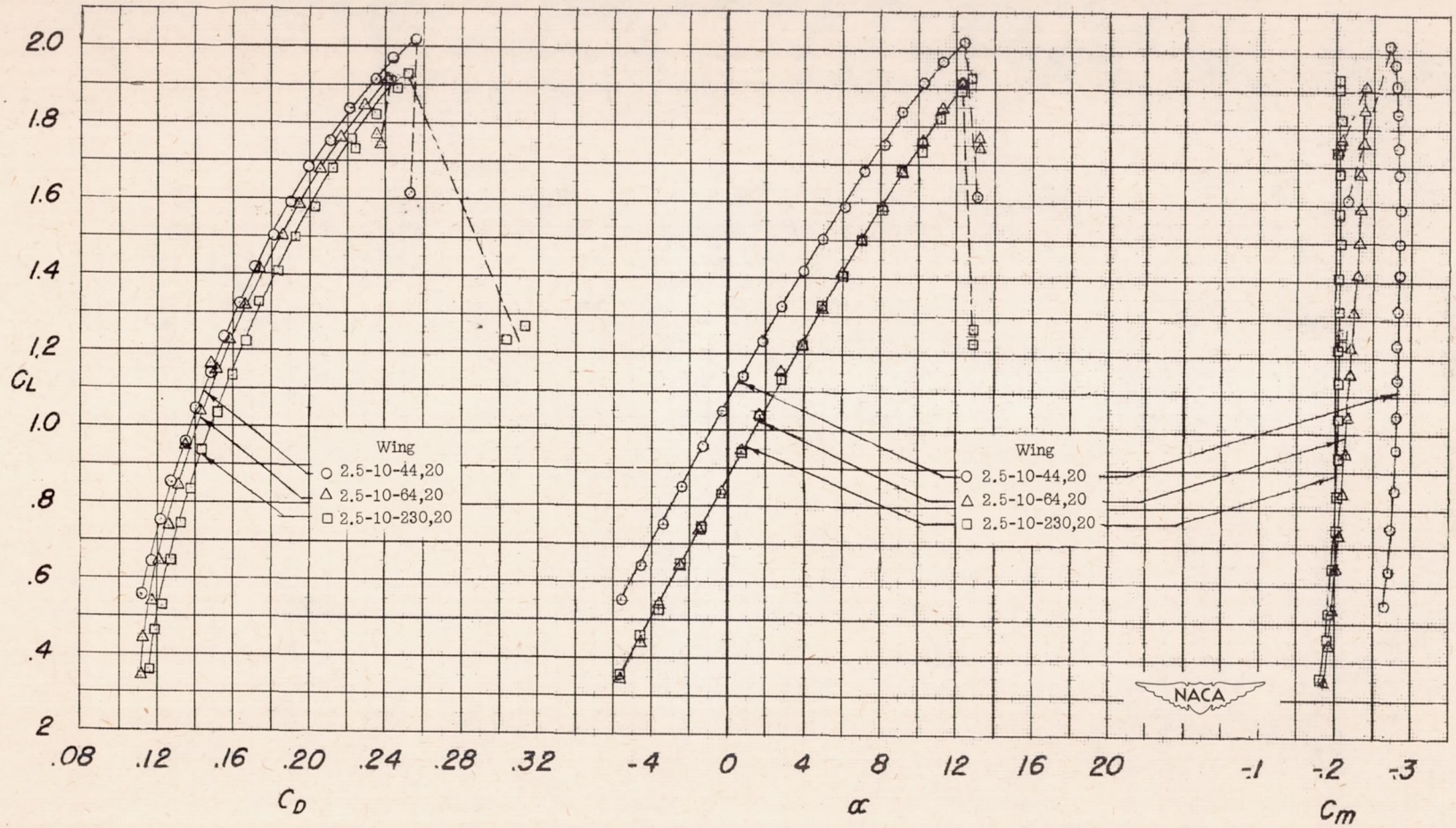

Figure 10.- Effect of airfoil section on the characteristics of wings with rough leading edge. Partial-span flaps deflected 60°; $R = 4.0 \times 10^6$.

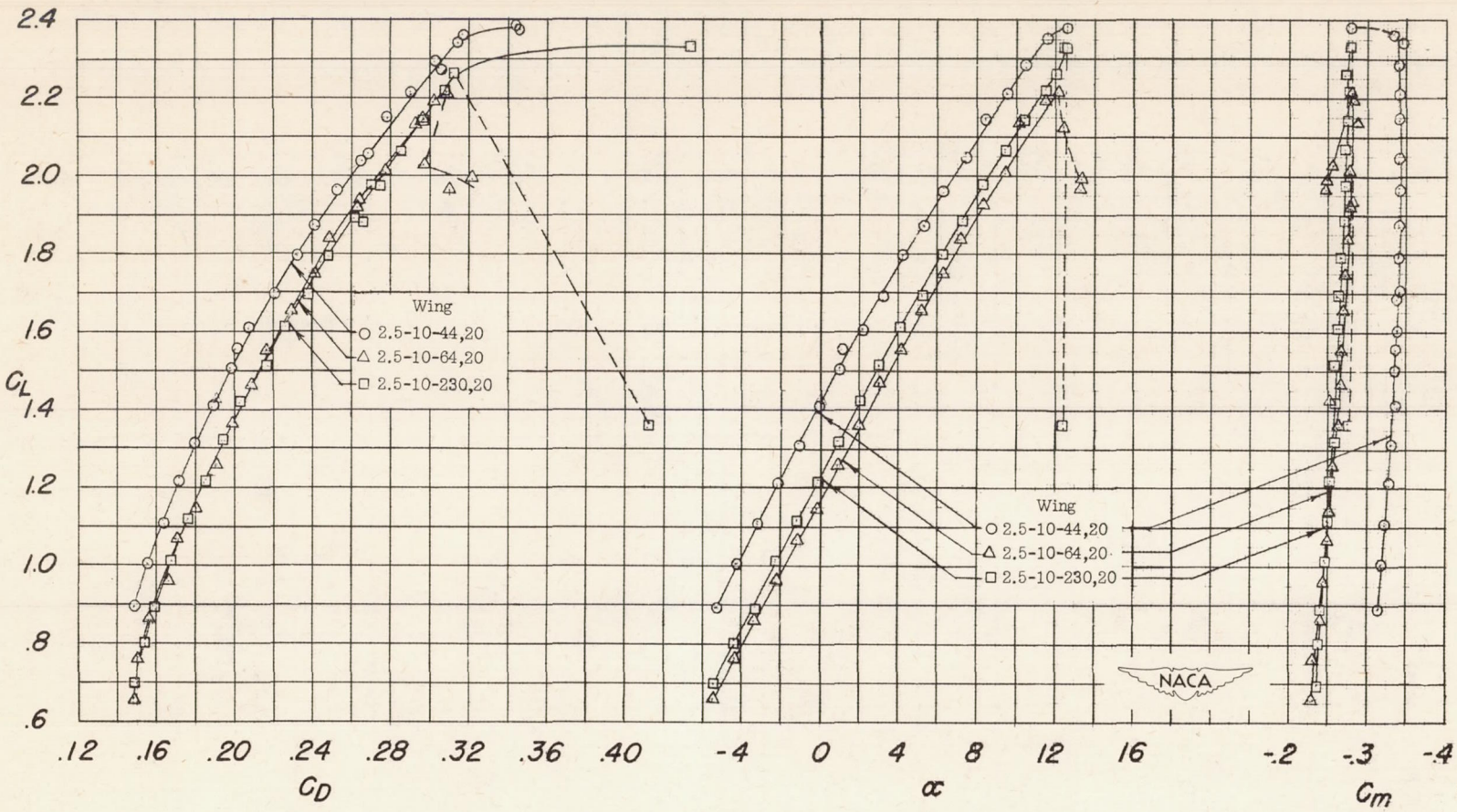

Figure 11.- Effect of airfoil section on the characteristics of wings with rough leading edge. Full-span flaps deflected 60°; $R = 4.0 \times 10^6$.

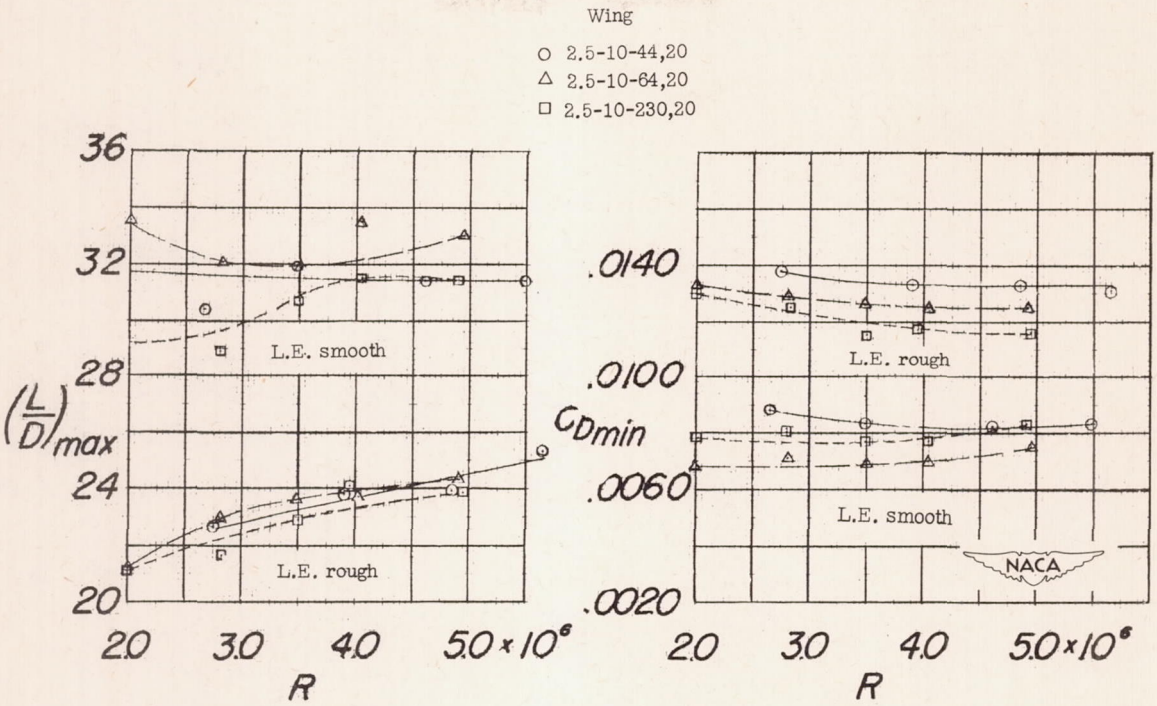

Figure 12.- Effect of Reynolds number on maximum lift-drag ratio and minimum drag coefficient of wings with smooth and rough leading edges.

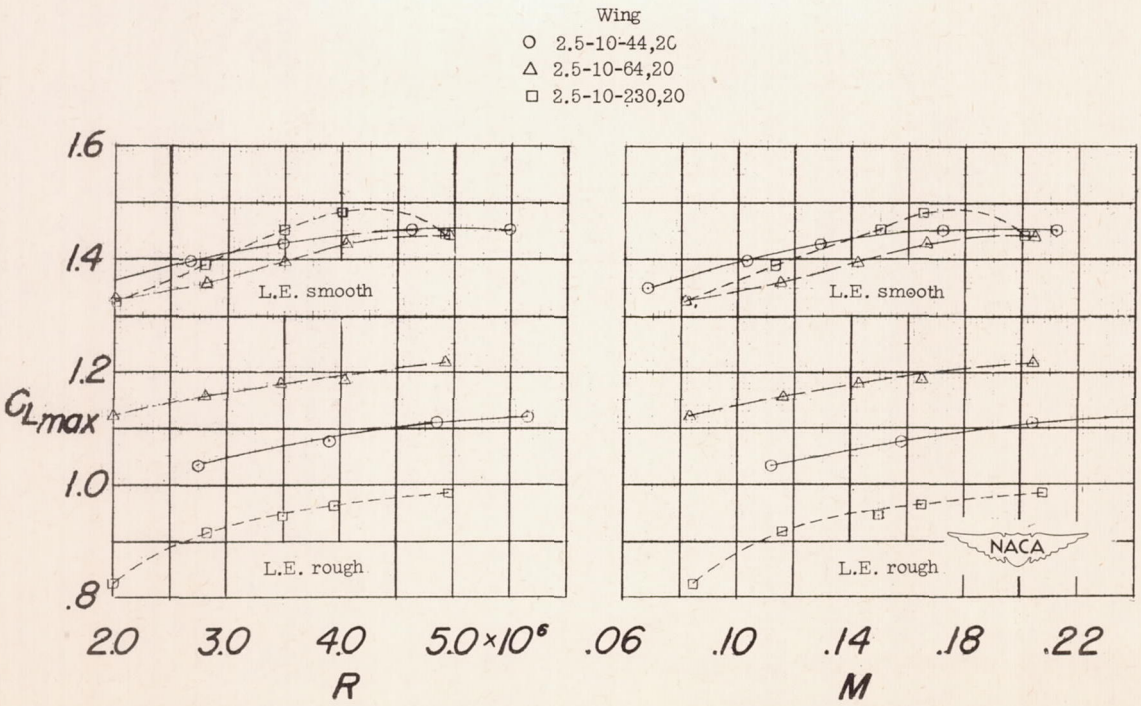

Figure 13.- Effect of Reynolds number on the maximum lift coefficient of wings with smooth and rough leading edges. Flaps neutral.

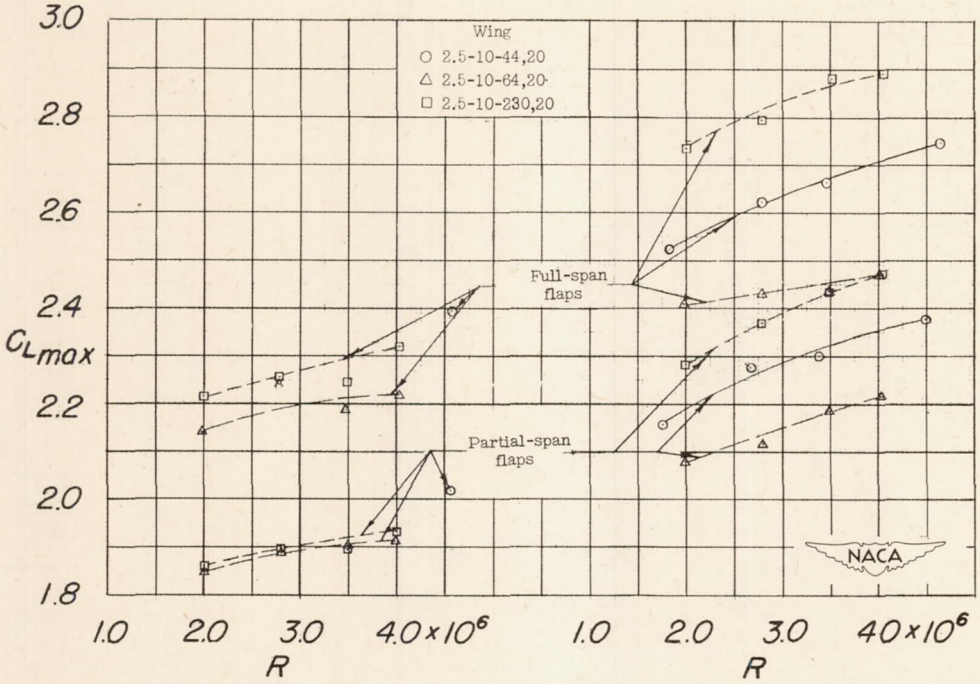

(a) Leading edge rough. (b) Leading edge smooth.

Figure 14.- Effect of Reynolds number on the maximum lift coefficient of wings with smooth and rough leading edges. Flaps deflected.

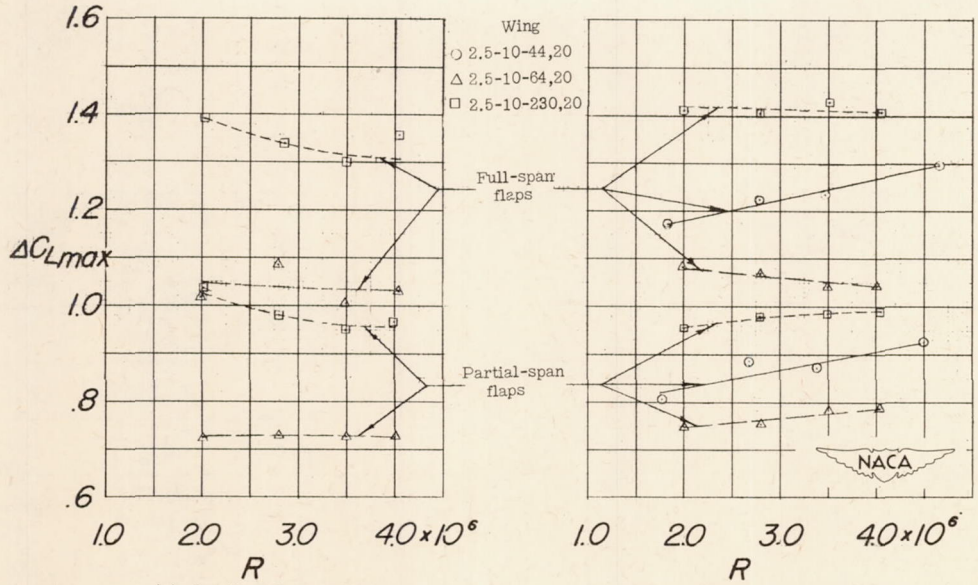

(a) Leading edge rough. (b) Leading edge smooth.

Figure 15.- Effect of partial-span and full-span flaps on the variation of the increment of maximum lift coefficient with Reynolds number for wings with smooth and rough leading edges.

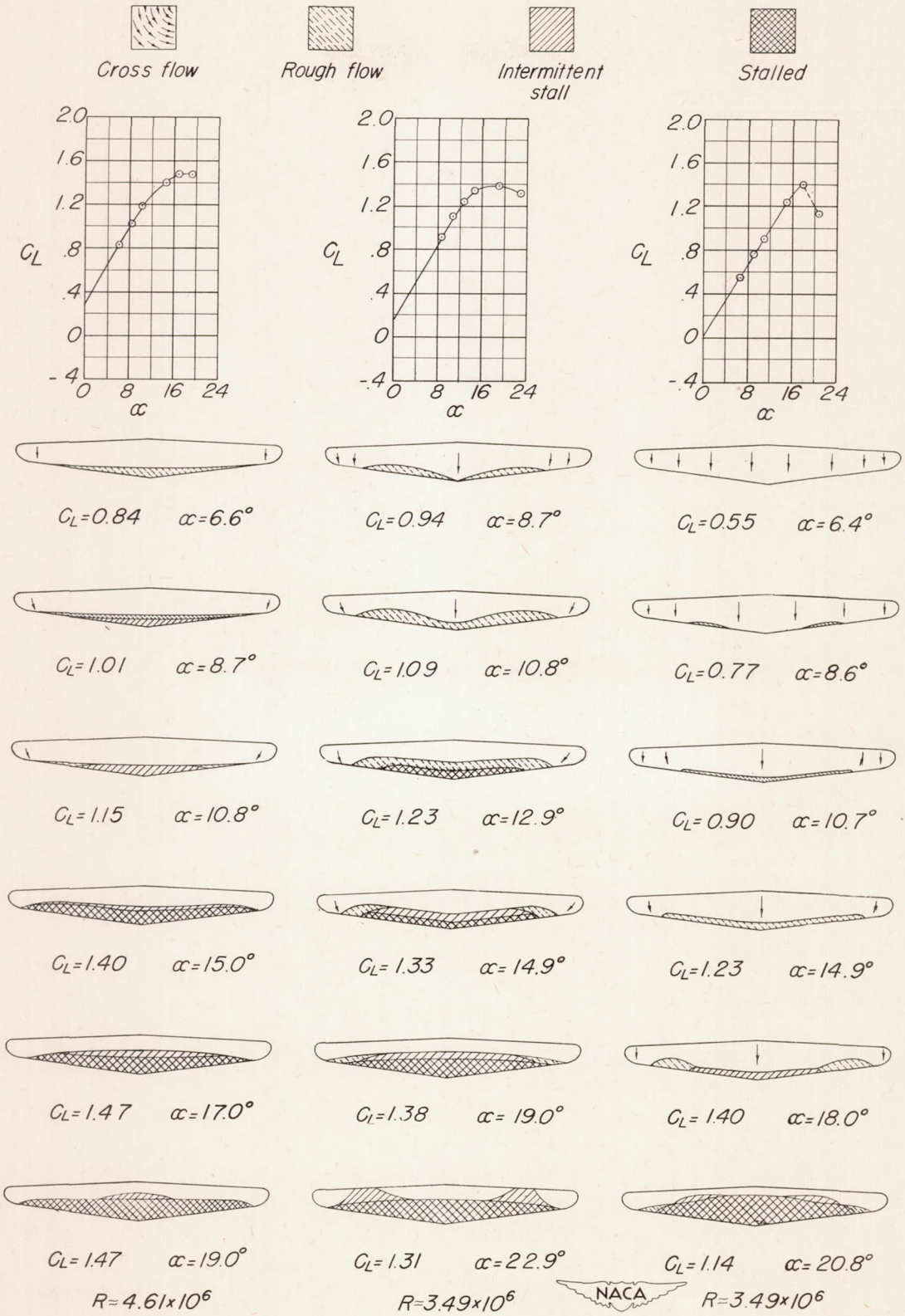

(a) Wing 2.5-10-44,20. (b) Wing 2.5-10-64,20. (c) Wing 2.5-10-230,20.

Figure 16.- Stall progression of wings with flaps neutral.

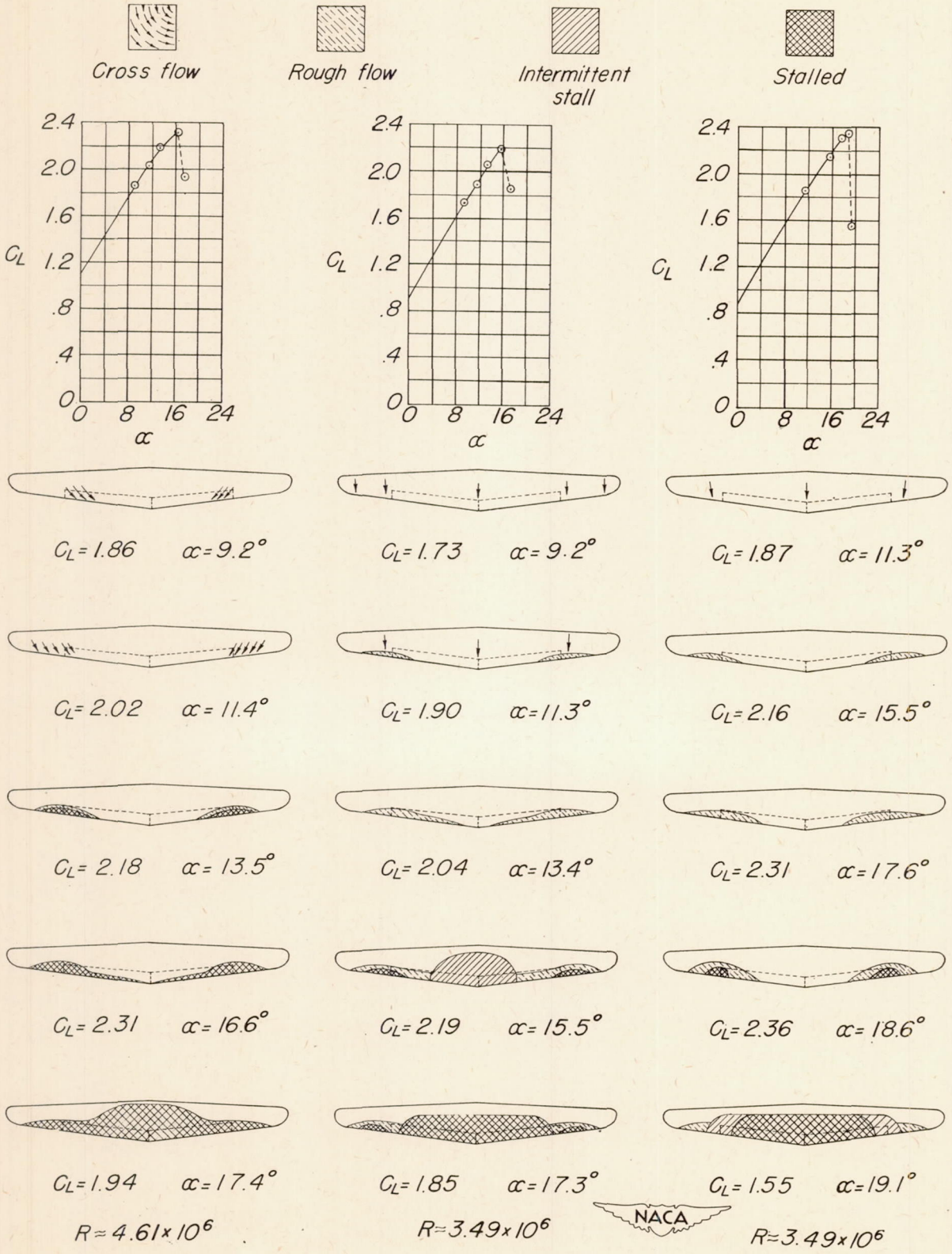

(a) Wing 2.5-10-44,20. (b) Wing 2.5-10-64,20. (c) Wing 2.5-10-230,20.

Figure 17.- Stall progression of wings with partial-span flaps deflected 60°.

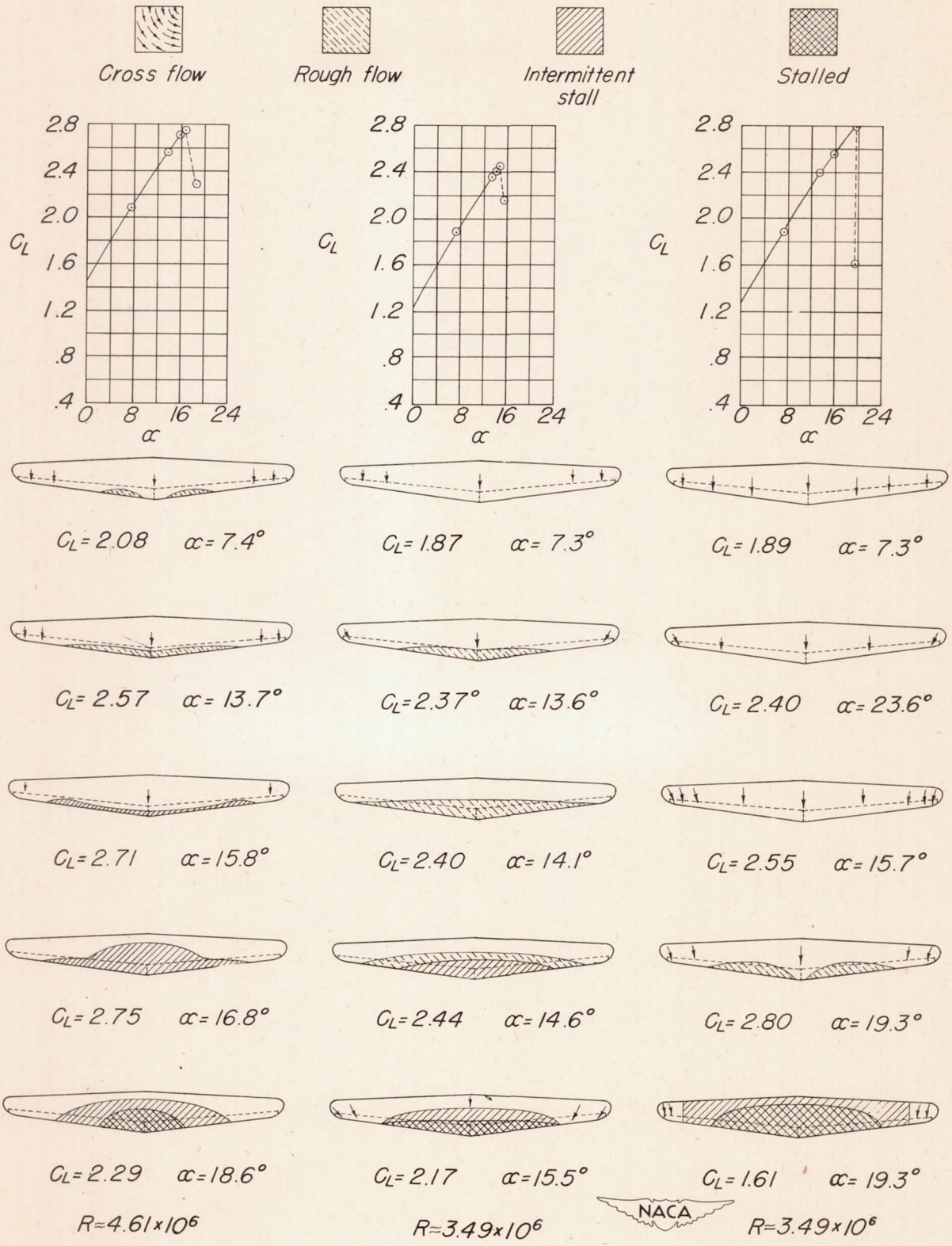

(a) Wing 2.5-10-44,20. (b) Wing 2.5-10-64,20. (c) Wing 2.5-10-230,20.

Figure 18.- Stall progression of wings with full-span flaps deflected 60°.